Neural Substrates of Chronic Pain in the Thalamocortical Circuit

Antonio G. Zippo[1], Riccardo Storchi[1], Maurizio Valente[1], Gian Carlo Caramenti[2], Gabriele E. M. Biella[1,]*

1. *Institute of Molecular Bioimaging and Physiology, National Research Council (CNR), Via Fratelli Cervi 93, 20090 Segrate (Milan), Italy*
2. *Institute Biomedical Technologies, National Research Council (CNR), Via Fratelli Cervi 93, 20090 Segrate (Milan), Italy*

**corresponding author (gabriele.biella@ibfm.cnr.it)*

Chronic pain (CP), a pathological condition with a large repertory of signs and symptoms, has no recognizable neural functional common hallmark shared by its diverse expressions. The aim of the present research was to identify potential dynamic markers shared in CP models, by using simultaneous electrophysiological extracellular recordings from the rat ventrobasal thalamus and the primary somatosensory cortex. We have been able to extract a neural signature attributable solely to CP, independent from of the originating conditions. This study showed disrupted functional connectivity and increased redundancy in firing patterns in CP models versus controls, and interpreted these signs as a neural signature of CP. In a clinical perspective, we envisage CP as disconnection syndrome and hypothesize potential novel therapeutic appraisal.

Chronic pain (CP) is a sensory disorder accompanying many pathological conditions with different modal, magnitude or temporal features (1). Though profuse analytical efforts and important findings, CP is still poorly understood because of its peculiar biological and clinical complexity (2). This is reflected in non-univocal relationships between intensity or modality and neural activation levels. Furthermore, unlike acute pain, CP is not necessarily sustained by inputs from the periphery, and it may even be free from any provoking causes (3). For instance, whereas spontaneous pain, allodynia and hyperalgesia may be mirrored by neuronal spontaneous hyperactivity or hyperresponsiveness (4,5,6) often, in CP, mutually inconsistent mosaics of brain area activations and inactivations (7,8) have also been described. Thus, neither actual linear intensity coding for CP, nor a necessary and sufficient common brain network activation clearly emerge (9,10). These questions interlace with general problems on brain default mode (11) and on issuing concepts of functional connectivity (12). Models for distributed representation of CP in the brain, like the Neuromatrix hypothesis (13) or the Homeostatic Model (14) diversely interpreted CP, yet as the result of integrative regional activities, which are active also in resting states. These works, however, give no hints on the way the neuronal brain substrates behave in the diverse CP conditions.

As the CP information, yet in its different manifestations, is carried by neuronal activities, it can be argued that some common neuronal feature may embody core markers of spontaneous CP. In this paper we identify some shared features of neuronal and network dynamics in spontaneous ongoing activity in experimental animal models of CP. Previous results, measured in our lab on the spinal cord, from simultaneously recorded dorsal horn neurons in superficial and deep spinal cord *laminae*, showed that a chronic constrictive neuropathy suppressed correlations among the two

layer neurons (15). This disordered, decorrelated source would project a misshapen input to the supraspinal stations, the first being the thalamus.

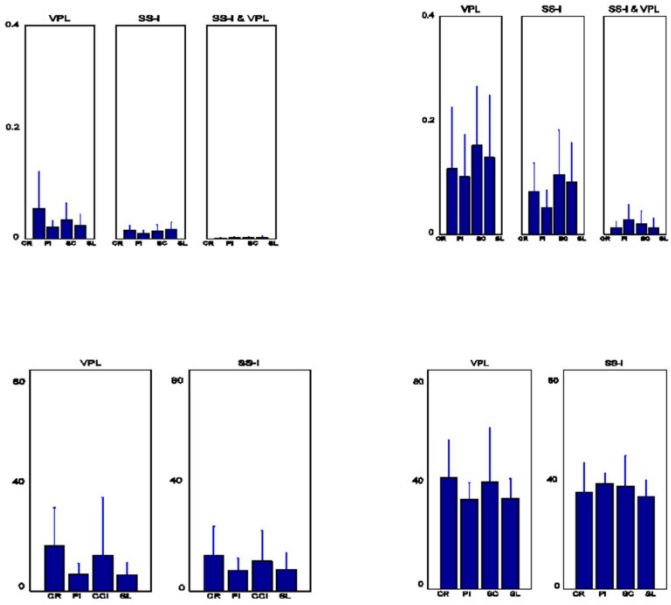

Figure 1. Above, average firing rate and Standard Deviation (SD) recorded on single units. Below, average firing rate and SD recorded on putative single cells. The values are slightly larger than what typically reported in literature, due to the choice of a conservative approach in cluster separation

On this evidence, we decided to explore potential rearrangements in the functional connectivity of the thalamo-cortical axis, likely to be affected by the decorrelated inputs in CP.

To address the point, we carried out experiments (20 Control, CR, and 30 CP rats, subdivided in three different models CP-1, CP-2 and CP-3, respectively an inflammatory, the Seltzer and the Bennett-Xie models (16).
Simultaneous electrophysiological extracellular recordings were performed on mildly Isoflurane-anesthetized rats, by using two matrix electrodes placed in the thalamus VB complex and in the Primary Somatosensory (SS-I) cortex. To get a preliminary picture of the basic properties of the ongoing activity, we estimated the firing rates and the correlations for single neurons. Firing rates and correlation coefficients both on single neurons and MUA were not significantly different between CR and CP animals, neither in thalamic nor in cortical neurons (Fig. 1). Thus we used statistical techniques able to detect long-range interactions and to estimate the information redundancy in the neuronal networks.
We assumed that each distinct firing pattern enclosed an individual message. Neurons sharing firing patterns are likely to convey reduced information because of the message redundancy, that we estimated by NCD (Normalized Compression Distance), a statistical technique detecting recurrent patterns and functional interactions (17).

Figure 2 displays four raster plots respectively sampled from CR and the three CP models.

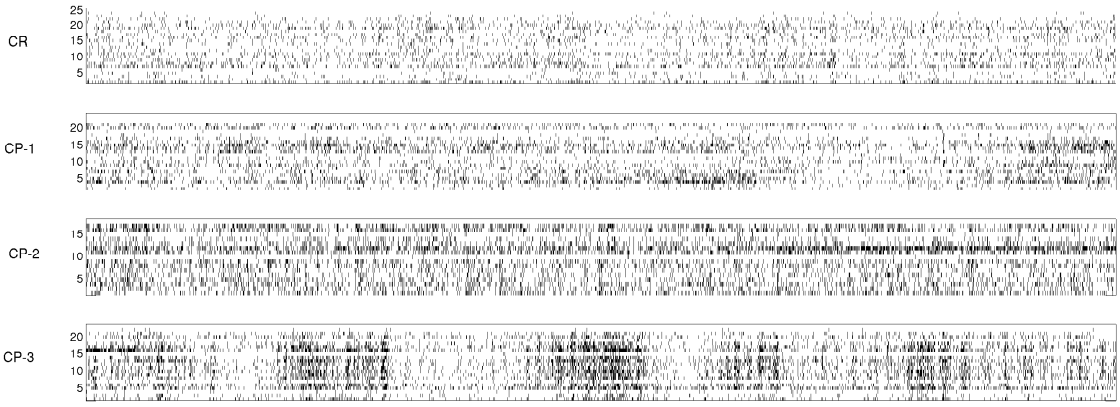

Figure 2. Raster plots representing 10 seconds of sampled activity from CR, CP-1, CP-2 and CP-3 models. In the y-axes are reported the recorded neurons. Plots are disposed with a redundancy increasing order.

Spike trains look more stereotyped (or redundant) in CPs than in CR. Thus, as expected, the estimated redundancies were up to 20.8% larger in CPs than in CR. These findings were consolidated by integrating redundancy of thalamus and cortex (Fig. 3). Additionally we computed the cross-redundancy on the thalamo-cortical axis. Again, we found that thalamo-cortical redundancy was significantly larger in CPs than in CR.

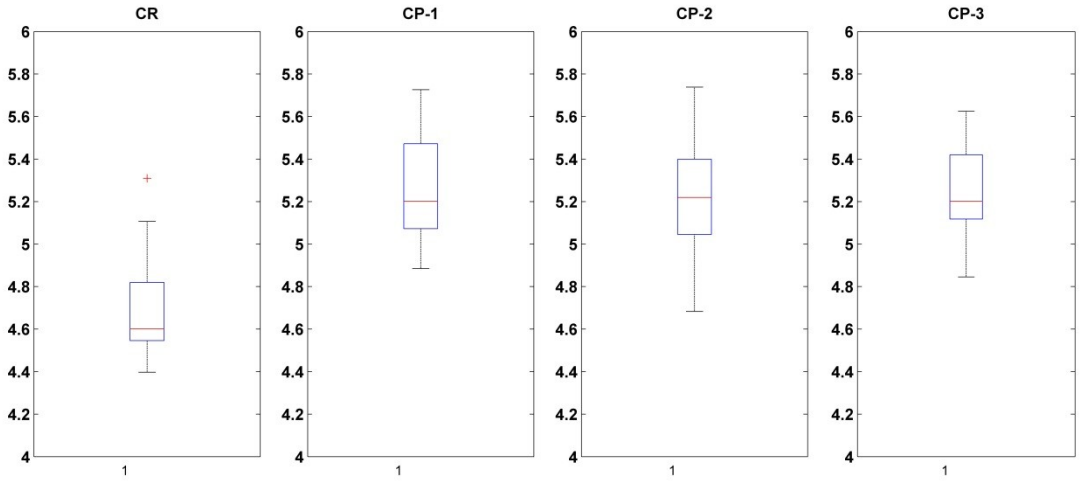

Figure 3. Thalamo-cortical redundancy (y-axes) in the four experimental conditions. CPs show significant increases of redundancy in comparison to CR ($P < 0.007$, ranksum test).

Firing pattern redundancies imply a functional coupling between neurons. By extracting these couplings, we built functional graphs among the recorded involved neurons. These graphs were

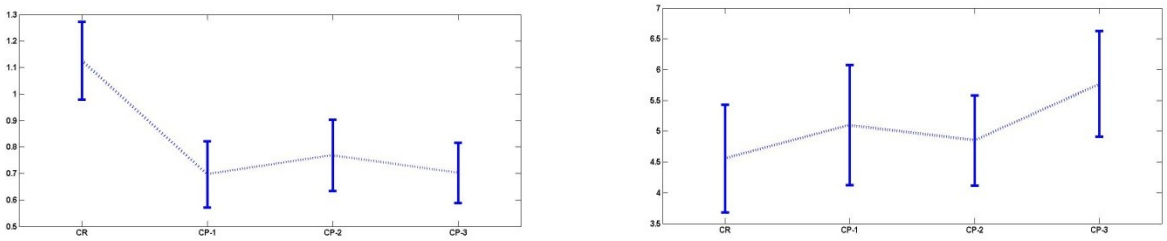

Figure 4. Left, transitivity estimated (y-axis) on the four experimental conditions. CPs show significant reduction of information integration (P < 0.001). Right, clustering coefficient estimated (y-axis) on the four experimental conditions. CPs show higher segregation of information (P < 0.004, ranksum test).

investigated by a specific statistic parametrization, namely by computing the *clustering coefficient* (measure of information segregation) and the *transitivity* (measure of information integration), that highlight the information transfer efficiency (18). Comparing these statistics, we found that the *clustering coefficient* was larger in CPs than in CR and, crucially, that the *transitivity* was smaller in CPs than in CR. In agreement with these findings, CR functional graphs, from ongoing neuronal activity, were small-world networks (19), while CP functional graphs lacked the necessary requirements for transitivity, thus not satisfying the requirements for small-world configurations. This indicates that in CP functional graphs, information transfer is less efficient, supporting the view of a disrupted functional connectivity in the CP models, that alters the small-world properties typical of CR (18).

In this work we effectively show that, in a regime of ongoing activity of the thalamo-cortical network, different animal models of CP homogeneously exhibit neural functional labels well distinguishable from those in control animals. However, these signs were not recoverable in immediately identifiable traits of the single unit (neuron) or network level (such as unit frequency increases, dysrhythmic patterns, or elementary correlations). Conversely, for all the models analyzed, remarkable differences were evident in the circuitry connectivity. Remarkably, the CP models shared comparable values of connectivity disorders in the thalamo-cortical circuit. More analytically, we could observe, as common markers of CP, greater information segregation, namely a higher degree of fragmentation in the small functionally co-active neuronal clusters, higher levels of pattern redundancy, and a dynamic feature well detected by special forms of graphs, known as small-world networks. As CP is a spontaneously active perceptual condition, thus leading to infer that its neural substrates are also active in resting states, we carried out our experiments exclusively on spontaneous activity conditions.

In the literature, in CP conditions, the presence of anomalously hyperactive neurons exhibiting tonic high-frequency discharges or dysrhythmic bursting, as well as sustained wind-up, activity-dependent plasticity disorders and receptor potentiation, has been repeatedly described in the spinal cord and, less extensively, in the thalamus or cortex (20, 21,22).

Preliminary analyses (Fig. 1) from our long-lasting recordings of ongoing spontaneous activity, showed no significant difference in the average spontaneous firing rate both of single neurons and of Multi-Units, yet in the presence of sparse and sporadic dysrhythmic or hyperactive neurons.

Dysrhythmic or hyperactive neurons may thus represent punctual results of a compromised situation, not producing however a relevant effect on the network. Such network-level effect would indeed be impeded by the energetic costs of hyperactivity, as metabolic constraints to neuron function are imposed by the conservation of a fixed energy budget (23), a condition hard to meet in very lasting pain conditions.

Recent fMRI observations on intrinsic brain connectivity in resting brain of patients with fibromyalgia showed a relation between connectivity disorders and chronic pain intensity (24). In an earlier study on intrinsic spinal cord functional connectivity in a neuropathy model, we reported a dramatic collapse of functional correlation between neurons in the superficial and deep spinal cord laminae (15). In our view, this input disorganization could project strongly anomalous signals to the supraspinal regions.

In our experiments, the functional connectivity anomalies in CP appear repetitive and stable and largely independent from background EEG spectral composition and from the anesthesia level (see Supplementary Material). Other data, on chronic pain subjects with thalamo-cortical dysrhythmia and increased coherence between the theta-beta EEG bands (20), or with peaks shifted towards low frequencies (25), are however not easily comparable with our findings. The redundancy increase in CP may be interpreted either as an emphasis of the relevant core of the message (e.g. noxious information, *per se*) or as a loss of system plasticity, compromising the local information flow. Because of the scarce evolutionary relevance of chronic pain (26), the hypothesis of "message rehearsal", as from redundancy, seems unlikely. The alternative hypothesis of a pathological sequence of events related to property loss appears therefore preferable. We conjecture that the rich array of neuronal configurations of normal animals can be explained by a major adaptability or plasticity.

Small-worldness appears more and more as a necessary property for the correct dynamics of complex brain networks (18). This indicates that the collapsed small-worldness in CP functional connectivity could be considered as the main reporter of disrupted or disordered functional connectivity.

Observations in psychiatric and neurodegenerative disorders suggested that functional disconnection might provide also a unifying conceptual substrate (27,28) for a number of pathologies strongly related to network dynamics. Disconnection, in the present context, does not necessarily mean an anatomical fiber disengagement but an altered functional connectivity architecture.

These results may help to understand data in the literature, which show that cortical or subcortical stimulations effectively reduce the perception of intractable pains (29,30). In fact, the delivery of timed inputs could functionally "rearrange" the disordered networks, thus reinstating some level of network efficiency.

Further investigations are now needed to explore the complex dynamics of neural activity in CP as the very substrate of such perceptual state. From a clinical point of view, they show the potential to open novel therapeutic paths based on opportunely tuned stimulations which, eventually in association with pharmacological approaches, may re-establish lasting conditions of effective functional connectivity.

References

1. Merskey H, Bogduk N, Classification of Chronic Pain, IASP Press, pp. 209-214 (1994).
2. Edward R. Perl Pain mechanisms: A commentary on concepts and issues Progress in Neurobiology, 94 20-38 (2011).
3. Grahek N, Feeling Pain and Being in Pain, Dissociation Phenomena in Human Pain Experience (A Bradford Book The MIT Press Cambridge) pp. 31-41 (2001).
4. Hao JX, Kupers R-C, Xu XJ, J. Neurophysiol., 92:1391-9 (2004).
5. J. M. Laird and F. Cervero J. Neurophysiol., 62(4):854-863 (1989).
6. Viswanathan A Freeman RD, Nat. Neurosci., 10:1308-1312 (2007).
7. Iadarola MJ et al, Pain, 63:55-64 (1995).
8. Baliki MN, Geha PY, Apkarian AV, Curr. Pain Headache Rep., 11:171-7 (2007).
9. Apkarian AV, Bushnell MC, Treede RD, Zubieta JK, Eur. J. Pain, 9:463-84 (2005).
10. Tracey I, British Journal of Anaesthesia, 101:32-9 (2008).
11. Raichle ME et al, Pro. Natl. Acad. Sci., 98:676-682 (2001).
12. Tononi G, Sporns O, BMC Neurosci., 4:31 (2003).
13. Melzack R, Pain, Suppl. 6:S121-6 (1999).
14. Craig AD, Ann. Rev. Neurosci., 26:1-30 (2003).
15. Biella G, Riva L, Sotgiu ML, Europ. J. Neurosci., 9:1017-1025 (1997).
16. Wang LX, Wang ZJ, Advanced Drug Delivery Reviews, 55:949-965 (2003).
17. Cilibrasi R, Vitanyi P, IEEE Trans. Information Theo., 51:1523-1545 (2005).
18. Bullmore E, Sporns O, Nat. Rev. Neurosci., 10:186-98 (2009).
19. Yu S, Huang D, Singer W, Nikolic D, Cereb. Cortex, 18:2891-2901 (2008).
20. Llinas RR, Ribary U, Jeanmonod D, Kronberg E, Mitra PP, Proc. Natl. Acad. Sci. USA, 96:15222-7 (1999).
21. Flor H et al, Neuroreport, 5:2593-7 (1994).
22. Florence SL, Taub HB, Kaas JH, Science, 282:1117-21 (1998).
23. Herculano-Houzel S, PLoS ONE, 6(3): e17514 (2011).
24. Napadow V et al, Arthritis Rheum., 62(8):2545-55 (2010).
25. Sarnthein J, Jeanmonod D, Neuroimage, 39:1910-7 (2007).
26. Williams AC, Behavioral and Brain Sciences, 25:439-488 (2002).
27. Mesulam MM, Brain, 121:1013-52 (1998).
28. Catani M, Mesulam M, Cortex, 44:911-3 (2008).
29. Gubellini P, Salin P, Kerkerian-Le Goff L, Baunez C, Prog. Neurobiol., 89:79-123 (2009).
30. Lefaucheur JP et al, Brain Stimul., 1:337-44 (2008).

Supporting Material

Electrophysiology

Fifty male albino rats (Sprague-Dawley, Charles River, Calco, LC, Italy, 270-350g) were chosen out of the set of the animals employed in the research.

The rats underwent preliminary barbiturate anesthesia for the surgical experimental preparation. The jugular vein and the trachea were cannulated to gain, respectively, a drug delivery pathway and the connection to the anesthesia-ventilation device. Before the placement of electrodes the rats were paralyzed by intravenous Gallamine thriethiodide (20 mg/kg/h) injection and connected to the respiratory device delivering (1stroke/s) an Isoflurane® 2.5% 0.4 to 0.8 l/min in Oxygen 0.15-0.2 l/min gaseous mixture. Curarization was maintained stable throughout the whole experiment by Gallamine refracted injections. During the experiment the anesthesia level was continuously monitored by the EEG recordings.

We simultaneously recorded spiking and local field potential activities from anesthetized rats, by two microelectrode matrices from three stations in the brain: the thalamic ventro-postero-lateral complex nuclei (VPL) and the primary somatosensory (S1) cortex. We also concurrently recorded from four EEG derivations. The neuronal electrophysiological recordings were obtained

contralaterally to the stimulated paw, the concurrent EEG recordings were obtained ipsilaterally to the stimulated paw.
The neuronal recordings were obtained by two matrices of extracellular tungsten or Pt-Ir electrodes were framed in 3x3 arrays of single shanks, inter-tip distance 150-200µm, tip impedance 0.5-1MΩ (FHC Inc., ME, USA).

EEG recordings

The EEG electrodes were placed along the stereotactic coordinates (in front-back order, Bregma as relative zero AP, zero ML reference point) as follows: FrontalAnterior (FA) +3 mm MedioLateral (ML) -2 mm, ParietalAnterior (PA) -0.15 mm, ML -2.8 mm, MiddleParietal (MP) -3 mm, ML. -3 mm, PosteriorParietal (PP) -6 mm, ML. -2.8 mm, reference in Occipital bone -9 mm, ML. 2 mm. [1]. For the analyses, we selected preferentially the EEG data from the second derivation placed over the sensory cortex mirroring the contralateral somatosensory primary cortex where the neuronal recordings were obtained.

Electrophysiological extracellular recordings

For the electrophysiological recordings, two holes were drilled on the skull of 3 mm^2 for the cortical and the thalamic matrix accesses. The holes were drilled centered respectively on the cortical access centered around a reference point at -1.5 mm AP and 2.5 mm ML, and the electrode was driven around 450 to 800 micrometer deep by an electronically controlled microsteppers (Narashige, Japan). The thalamic access hole was centered at -6 mm AP and -2.5 mm ML. The thalamic matrix was inserted with a slant at 25° and driven at least at 5500 micron in depth and then advanced electronically by a second electronically driven microstepper (Transvertex, Stockholm) until full responses were observed to peripheral test stimuli. Fast thalamic and cortical responses to light tactile stimuli with a brush-test on the sciatic innervation field (the plantar aspect of the left hindlimb) were the anatomo-functional acceptance criteria for acquisition. All the experimental blocks were organized with periods of ongoing activity recordings lasting around 20 min. and not more to preserve at most the data homoscedasticity, in the additional stable conditions of gaseous anesthesia. After a cycle of spontaneous and stimulated activities was completed, we repeated twice the original recordings. Then we advanced in depth the electrodes, 20µm and 100µm respectively for the cortical probe and the thalamic matrix ensemble, to reach an adjacent region, then checking again with the test stimulus the responsiveness of the newly recorded regions. In positive cases we repeated the recording cycle as above. We recorded from five to six stations in progressive steps for each animal.
For signal amplification and data recordings a 32 channel Cheetah Data Acquisition Hardware was used (Neuralynx, MT, USA, sampling frequency 32 kHz). Electrophysiological signals were digitized and recorded with bandpass at 6 kHz and 300 Hz for spikes and at 475 Hz-1 Hz for the EEG. The data stored were analysed off-line both by Matlab and by locally developed softwares. A histological confirmation of the placement of the electrodes was then obtained on brain coronal sections stained with cresyl-violet.
All the animals have been treated along the Italian and European Laws on animal treatment in Scientific Research (Italian Bioethical Committee, Law Decree on the Treatment of Animals in Research, 27 Jan 1992, No. 116). The National Research Council, where the experiments have been performed, adheres to the International Committee on Laboratory Animal Science (ICLAS) on behalf of the United Nations Educational, Scientific and Cultural Organizations (UNESCO), the Council for International Organizations of Medical Sciences (CIOMS) and the International Union of Biological Sciences (IUBS). As such, no protocol-specific approval was required.

Variable Order Markov Models

Lossless compression algorithms model symbolic sequences in order to produce new shorter encoded sequences. In a first stage, these algorithms deliver a probabilistic model of a sequence and adopt the model probabilities to encode the new shorter sequence. To build the probabilistic model, the algorithm identifies recurrent variable-length patterns of symbols within the sequence. Many lossless compression algorithms perform the probability estimations by modeling the sequence through Variable Order Markov Models (VOMMs) [5]. This allows for modeling time dependencies between the sequence symbols up to a maximum fixed order *k*. Our symbolic sequences of neurophysiological data (LFP phases and spikes) extracted by time windows of 50-100 ms were implicitly modeled by VOMMs choosing a value for *k* fixed to half of the time window size. We took into consideration two efficient lossless compression algorithms: the Prediction by Partial Matching (PPM) [6,7] and the Context-Tree Weighting (CTW) [8,9].

Compression based similarity function

Similarities between sequences of spike occurrences were estimated by a function based on compression algorithms called Normalized Compression Distance (NCD) [10,11,12].
Formally, given that *x* and *y* are two signal sequences (e.g. spike trains or LFP phases), the NCD is defined as follows:

$$NCD(x,y) = 1 - \frac{C(x \cdot y) - \min(C(x), C(y))}{\max(C(x), C(y))}$$

where the *C* function represents the compressed sequence length and $\cdot$ is the sequence concatenation operator. If *NCD(x,y)* is equal to 1, the sequences *x* and *y* are considered similar. If equal to 0, the sequences are profoundly dissimilar.
Current analyses yet capturing synchronous firing patterns miss, however, common non-synchronous ones [13,14]. Non-synchronous patterns (in the range of few tens of milliseconds) can indeed represent more complex or long range interactions. We therefore employed the NCD function, able to measure the similarity of spiking sequences detected in time windows assuming that high values of similarity correspond to actual functional connectivity relationship.
We remark that the NCD function is a feature-free distance function, i.e. the similarity estimation is not based on some fixed features. On the contrary, many other similarity measures are feature-based, namely requiring detailed context knowledge. As a rule, the NCD function is asymmetric, i.e. $NCD(x,y) \neq NCD(y,x)$, i.e. *x* may contain more *y*-patterns than the reverse.
By the NCD function we estimated the functional connectivity between neurons as expressed by their spike sequences. We first split each sequence into equal-length time windows and then we computed the NCD matrix for all neurons. The resulting NCD matrices took values in the range [0,1]. We repeated the analyses with different window sizes from 50ms to 1s. A fixed threshold selected the strongest connections allowing for the construction of the functional connectivity direct graph. Formally the functional connectivity of neurons was represented by the graph G = (V,E) where V and E express, respectively, neuron and functional connection sets. For instance, if *x* and *y* represent the spike sequences of two distinct neurons with *NCD(x,y)* = 0.87, then a connection $x \rightarrow y$ is established.

Small-World Networks

A small-world network is obtained by evolving a basic graph where each node is connected to each neighbor. The chosen neighborhood involves typically much less nodes than the total node number $(N \gg K \gg \ln(N) \gg 1)$. The graph evolution is achieved by randomly adding and removing edges from the starting graph [20,21].

The resulting graph has many, typically small, quasi-complete subgraphs (cliques) where each node is connected to every other clique node. Again small-world networks exhibit short average distances between nodes.

From a functional perspective, small-world networks can express two important information processing features: information integration and segregation [22]. Functional segregation allows for specialized processing within densely interconnected nodes (cliques). Functional integration allows for combining information processed in distributed nodes or cliques. These network properties can be measured by two statistics: the clustering coefficient (C) and the characteristic path length (L) [20,23].

Formally, let G be a graph represented by the adjacency matrix $A = a_{ij}$ where $i,j \in N = \{1, \dots, n\}$ the set of nodes. We define the measure C as

$$C = \frac{1}{n} \sum_{i \in N} \frac{2t_i}{k_i(k_i - 1)}$$

where t_i is defined by

$$t_i = \frac{1}{2} \sum_{j,h \in N} a_{ij} a_{ih} a_{jh}$$

and k_i is the degree of the node *i*. We also define the measure L as

$$L = \frac{1}{n} \sum_{i \in N} \frac{\sum_{j \in N, j \neq i} d_{ij}}{n - 1}$$

where d_{ij} is the shortest path length between nodes *i* and *j*. Finally, it is possible to combine both measures in order to obtain a global small-worldness measure (S) as

$$S = \frac{C/C^r}{L/L^r}$$

where C^r and L^r are computed on random networks with the same connection density of the experimental ones. Graphs are considered small-world networks whether $S \gg 1$ and $\frac{L}{L^r} > 1$.

References

1. Lu XC, Williams AJ, Tortella FC (2001) Quantitative electroencephalography spectral analysis and topographic mapping in a rat model of middle cerebral artery occlusion. Neuropathology and Applied Neurobiology 27, 481-495.
2. Montemurro MA, Rasch MJ, Murayama Y, Logothetis NK, Panzeri S (2008) Phase-of-firing coding of natural visual stimuli in primary visual cortex, {\it Current Biology}, 18(5): 375-380.
3. Zanos TP, Mineault PJ, Pack CC (2010) Removal of spurious correlations between spikes and local field potentials, J. Neurophysiol., published ahead. doi: 10.1152/jn.00642.2010.
4. Quiroga RQ, Nadasdy Z and Ben-Shaul Y (2004) Unsupervised spike sorting with wavelets and superparamagnetic clustering. Neural Computation 16:1661-1687.

5. Begleiter R, El-Yaniv R, Yona G (2004) On Prediction Using Variable Order Markov Models. Journal of Artificial Intelligence Research, 22:385-421.

6. Cleary J, Witten I (1984) Data Compression Using Adaptive Coding and Partial String Matching. IEEE Transactions on Communications, 32(4):396-402.

7. Teahan W (1995) Probability estimation for PPM. Proceedings of the New Zealand Computer Science Research Students' Conference, University of Waikato, Hamilton, New Zealand.

8. Willems F, Shtarkov Y, Tjalkens T (1995) The Context Tree Weighting Method : Basic Properties. IEEE Transactions on Information Theory 41(3):653-664.

9. Willems F (1998) The Context-Tree Weighting Method: Extensions. IEEE Transactions on Information Theory 44(2):792-798.

10. Sculley D, Brodley CE (2006) Compression and Machine Learning: A New Perspective on Feature Space Vectors. Proceedings of Data Compression Conference (DCC'06).

11. Cilibrasi R (2007) Statistical Inference through Data Compression, PhD Thesis at Institute for Logic, Language and Computation Universiteit van Amsterdam, ILLC Dissertation Series.

12. Cilibrasi R, Vit\'anyi P (2005) Clustering by Compression. IEEE Transactions on Information Theory 51:1523-1545.

13. Yu S, Huan D, Singer W and Nikolic D (2008) A small World of Neuronal Synchrony. Cerebral Cortex 18:2891-2901.

14. Schneidman E, Berry MJ, Segev R, Bialek W, Weak pairwise correlations imply strongly correlated network states in a neural population, {\it Nature}, 440:1007-1012 (2006).

15. Fries P (2005) A Mechanism for Cognitive Dynamics: Neuronal Communication Through Neuronal Coherence. Trends Cogn Sci. 9:474:480.

16. Womelsdorf T, Schoffelen JM, Oostenveld R, Singer W, Desimone R et al (2007) Modulation of Neuronal Interactions Through Neuronal Synchronization. Science 316:1609-1612.

17. Canolty RT, Ganguly K, Kennerley SW, Cadieu CF, Koepsell K et al (2010) Oscillatory phase coupling coordinates anatomically dispersed functional cell assemblies. Proceedings of the National Academy of Science USA 107:17356-17361.

18. Latham PE, Lengyel M (2008) Phase Coding: Spikes Get a Boost from Local Fields. Current Biology 18(8):349-351.

19. Pereda E, Quiroga RQ, Bhattacharya J (2005) Nonlinear multivariate analysis of neurophysiological signals. Progress in Neurobiology 77:1-37.

20. Watts DJ and Strogatz SH (2009) Collective dynamics of 'small-world' networks. Nature 393:440-42.

21. Albert R, Barab\'asi (2002) Statistical Mechanics of Complex Networks. Reviews of Modern Physics 74:47-97.

22. Edelman GM , Tononi G (2000) A Universe Of Consciousness: How Matter Becomes Imagination. Basic Books.

23. Rubinov M, Sporns O (2010) Complex network measures of brain connectivity: Uses and interpretations. Neuroimage 52(3):1059-1069.